44th Annual CNS Conference and the 49th Annual CNS/CNA Student Conference
Westin Harbour Castle Hotel, Toronto, ON, Canada, June 8-11, 2025

ANALYSIS OF LOCAL POWER AND FUEL COMPOSITIONS FOR A FUEL BUNDLE USED IN A REFITABLE PRIMARY HEAT TRANSPORT SYSTEM FOR PHWRs

I. Attieh[1] and R. I. Lounsbury[2]
[1]Attieh Nuclear Innovations Inc., Mississauga, Ontario, Canada
[2]Suretech Development Limited, Deep River, Ontario, Canada

ibrahim@ani.engineer, lounsbur@sdl.on.ca

Abstract

The power output of current Pressurized Heavy Water Reactors (PHWRs) can be doubled by refitting them with a super-critical heavy-water (SCHW) primary heat transport system (PHTS) [1]. The refit involves replacement of the PHTS, fuel channels' and fuel bundles' material with materials that can operate at higher temperatures than the existing PHWRs. The new fuel cladding material, single crystal sapphire, requires careful control of local power distributions to avoid fuel pellet clad interaction (PCI) during normal operation and accident conditions.

This paper describes a detailed MCNP model of half a bundle of the SCHW reactor. This model predicts radial and axial fuel composition and power distribution as a function of fuel burnup, from fresh fuel to exit irradiation. The model is based on high fidelity constructive geometry modelling in MCNP6.3™, to capture the end-flux and power peaking at the endplate region and power distribution within the fuel pins as a function of burnup. The model provides insights into features that are unique to the refit reactor fuel, such as the use of two enrichments to limit local fuel power caused by end flux peaking and the use of Inconel springs to control fuel pellet gap spacing due to fuel cladding irradiation expansion and reduce local pellet power at the end region.

1. Introduction

The demand for electricity in North America is increasing as a result of increased electrification of industry, transportation and heating and artificial intelligence facilities. In eastern Canada, the primary focus for new generation is nuclear power, increased hydraulic generation, wind generation with natural gas for demand peaks. While large scale new nuclear generating stations are being investigated and built, they have long lead times. Another option is to examine ways to get significantly more power from existing PHWR / CANDU nuclear generating stations.

The power output of existing PHWR / CANDU type plants can be doubled through a modular replacement of the primary heat transport system (PHTS), fuel and fuel channels and fueling machines [1,2,3]. These systems will have higher temperature (max 625 °C) and pressure (Max. 25 MPa) for higher output and thermal efficiency. These system replacements are hereafter

referred to as a PHWR refit. There are several advantages to obtaining increased nuclear generating capacity through refitting existing PHWR / CANDU plants:

- The construction time is much shorter than that of large plant new builds (3 versus 10 years)
- No new site is required, thereby enhancing land use and simplifying approvals
- Project management relies on methods proven during refurbishments
- No new operating organization is required

The PHWR refit has only a slightly increased number of components compared to existing PHWRs. With double the power output, per MWh operating and maintenance costs will improve over existing PHWRs. Updated versions of large power reactors (e.g. EPR, AP-1000) require long new build construction times and have encountered significant cost and schedule overruns on their first plants. The PHWR refit can be constructed in much shorter times while benefitting from project management experience developed during PHWR refurbishment.

The PHWR refit relies on different in-core materials than existing PHWRs to allow higher temperature and pressure operation. A key new material is single crystal sapphire fuel cladding [2]. While this material performs well at high temperature, and in irradiation environments, it deforms only elastically in the normal operating range. This is quite different than the existing reactor zircalloy-4 sheath material. One implication is that fuel pellet cladding interaction (PCI) becomes a key operating limit. Localized power effects, such as bundle to bundle end flux peaking and fuel radial power distribution can influence PCI. This requires a detailed reactor physics evaluation of the fuel bundle to predict local powers.

2. Limitations of The CANDU Reactor Physics Industry Standard Toolset

The Reactor Physics Industry Standard Toolset (IST), that has been approved by the Canadian Nuclear Industry for modelling, has limitations that prevents it from modelling the SCHW reactor properly. It is based on WIMS-AECL, RFSP-AECL and DRAGON. WIMS-AECL is a 2-D lattice physics code that was originally develop in the UK and later at the Chalk River Laboratory. RFSP is a diffusion code that was developed by AECL. DRAGON is a 3-D transport code that is utilized by the industry to create incremental cross-sections to model the reactivity devices in RFSP.

The 2-D lattice physics calculations in WIMS-AECL cannot model the 3-D variations in the fuel composition in the SCHW reactor fuel bundle and the springs and washers in neither the fresh fuel composition nor as a function of burnup. Furthermore, the diffusion code, RFSP-AECL homogenizes the WIMS-AECL lattice cross-sections over the full bundle such that no detailed fuel-pin detailed information could be retrieved from the full-core calculations.

These limitations necessitate the utilization of the Monte Carlo N-Particle 6.3™ (MCNP6.3™) transport code to solve the transport equation in 3-D as a function of burnup. MCNP6.3™ is a Monte-Carlo method-based code that solves the transport equation in 3-D. The code has been under development by Los Alamos National Laboratory since the Manhattan Project. MCNP6.3 is the gold-standard for solving the neutral and charged particles transport equation. Its

limitations are that it demands significant computational resources. For this reason, it is used as benchmarking tool for other codes as opposed to being a design and analysis tool. However, as computational resources become more powerful and less expensive, MCNP6.3™ is being utilized more as a design tool.

The advantages of MCNP6.3™ is that it models the problems' geometry with high fidelity. Until recently, any geometry could be modelled with constructive geometry, which is a Boolean combination of first order and second order surfaces. Recently, unstructured mesh capabilities have been added to MCNP6.3™, which allows the modelling of any problem based on the original CAD model. Theoretically, with high fidelity modelling of geometry and material composition, MCNP6.3™ could replicate reality. However, there are always uncertainties in the materials neutronic cross-sections, which limit the fidelity of the obtained solution.

3. Modelling the SCHW Reactor Fuel Bundle in MCNP6.3™

The SCHW reactor bundle geometry is based on the 43-element CANFLEX model. However, due to the use of slightly enriched fuel and higher fuel burnup, the SCHW bundle has a more complex configuration. To suppress the power peaking at the end-regions of the bundle, two natural uranium pellets are at either end of each fuel pencil. To accommodate the expansion of the fuel cladding due to irradiation, two washers and one spring are located between the fuel pellets at either end of each fuel pencil, as outlined in this paper.

This paper outlines the modelling of SCHW half-bundle in a forward channel to capture the variations in the k-infinity, fuel burnup, power distribution, end-flux peaking, and gas production in the half-bundle model. This is a preliminary bundle model that could be refined further by varying the fuel temperature within each fuel pencil, varying the coolant temperature and density along the bundle, etc.

3.1 Modelling of the Non-Fuel Elements Components of the Bundle

The non-fuel elements of the bundle lattice, such as the moderator, pressure tube, insulator tube, coolant, cladding, endcaps, and gap between the insulator tube and pressure tube are modelled with high geometric and materials specifications fidelity. The radial cross-sectional view of these elements in the MCNP6.3 model are shown in Figure 1. The axial cross-sectional view of these elements is shown in Figure 2. The modelling of the endplates and the washers is shown in Figure 3 and 4, respectively. The design of the endplates has not been finalized. However, to preserve the mass and volume of the endplates, they were modelled as three concentric tubes. They will be modelled with higher fidelity once their design is finalized.

All these components could be seen in the axial cross-section view in the bundle, as shown in Figure 5. The springs and washers can be seen in the cross-section view. The springs have the bigger gap to accommodate the axial expansion of the fuel cladding as a function of cladding fast neutron fluence. The endcaps and endplate could also be seen in Figure 5. The segmentation of fuel elements will be discussed in the next section.

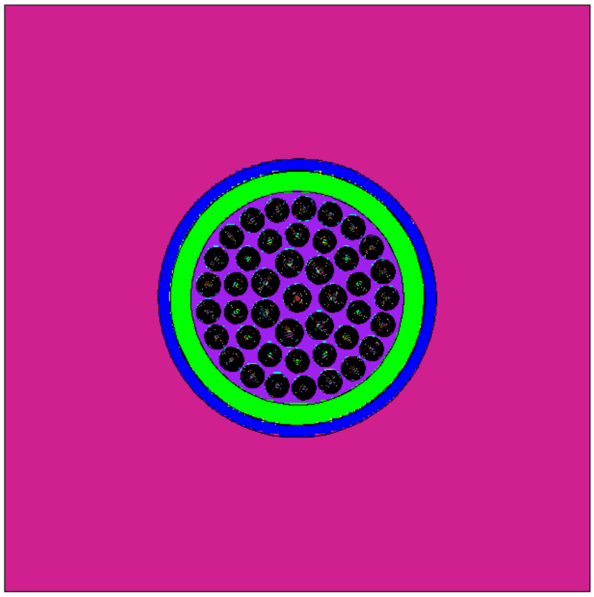

Figure 1: Radial Cross-Sectional View of the SCHW bundle in the MCNP Model

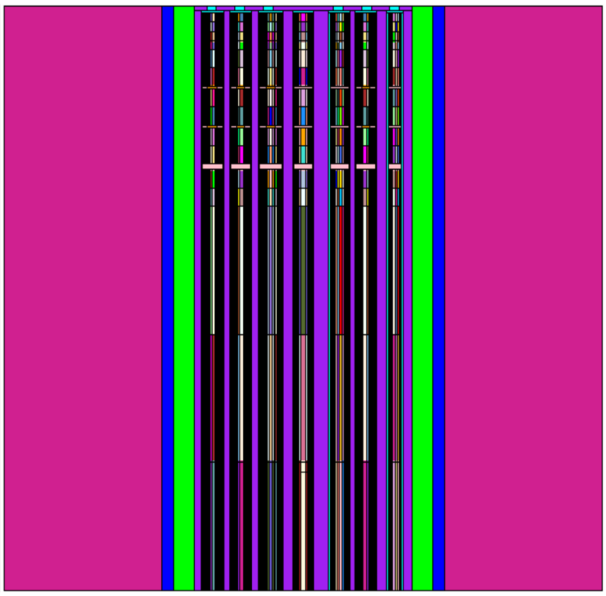

Figure 2: Cross-Sectional View of the SCHW Half Lattice MCNP Model in the Axial Direction

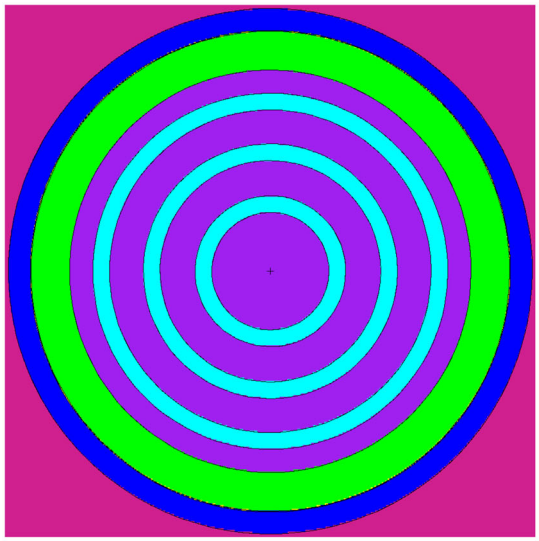

Figure 3: Modelling of the Endplates in MCNP Model

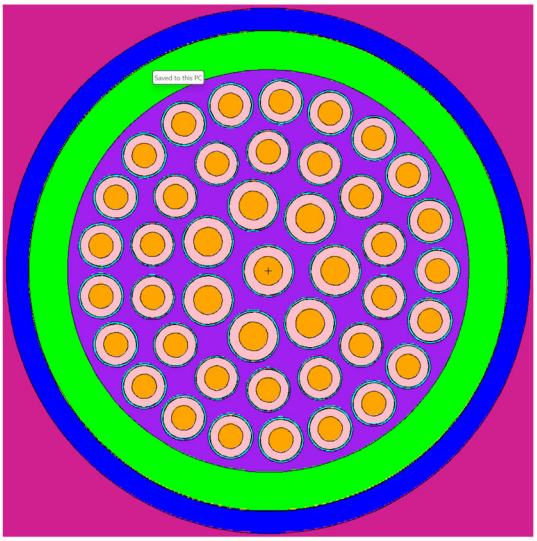

Figure 4: Modelling of the Washers in MCNP

3.2 Geometric Specifications for the Fuel Pencil

The geometric specifications for the fuel pencil have been complicated by the presence of the spring and washers and the need to segment the fuel elements for burnup calculations. The segmentation of the fuel will allow for the capturing of the impact of the end-flux peaking on the power distribution in the bundle. Furthermore, there are two natural uranium pellets in each fuel pencil at either end of the fuel pencil to suppress the flux peaking at the endplate regions.

Finally, the springs and washers are made from Inconel, which is a strong neutron absorber. This high neutron absorption will suppress the thermal flux in their proximity and impact the fuel burnup. Besides the segmentation of the fuel pellets in the axial direction, the fuel pellets are segmented in the radial and azimuthal directions to capture the radial and angular variations within each fuel element and within the bundle itself.

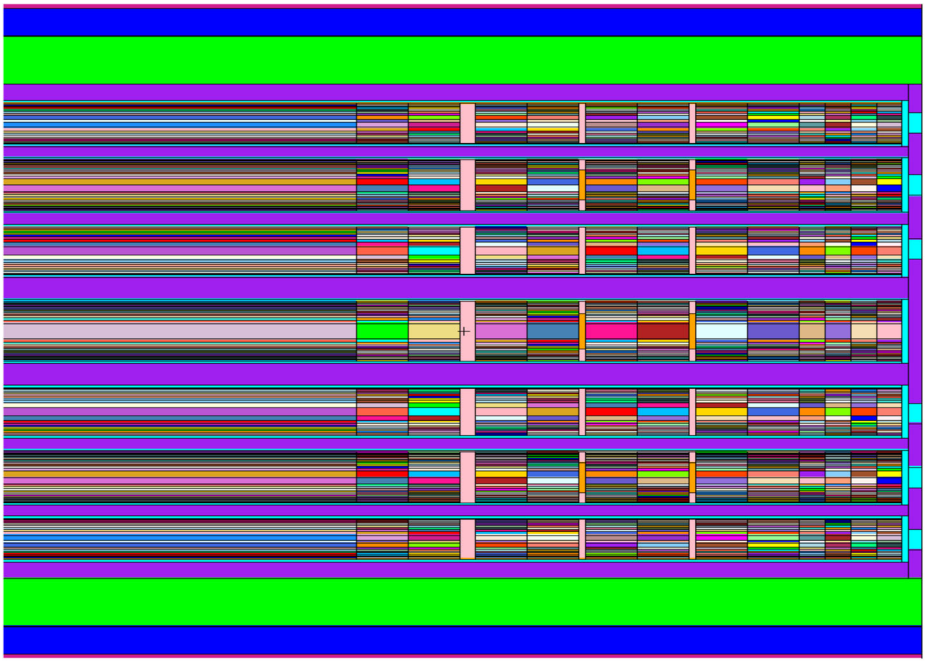

Figure 5: Cross-Sectional View of the Springs, Washers, Endcaps, and Endplates in MCNP

From Figure 6, the fuel elements are segmented into two segments in the angular direction. One segment is facing the center of the bundle, and the other segment is facing the opposite direction. This angular segmentation is to capture the variation in the flux in the radial direction, from the centre of the bundle to the periphery of the lattice.

The radial segmentation is to capture the flux and burnup variations within the fuel elements themselves and within the bundle. The flux varies significantly within the fuel elements themselves. Furthermore, there is a skin-effect that is captured using radial segmentation.

Each pin is segmented into two angular and fifteen radial segments, for a total of thirty segments. To capture the skin effect, the radius for each segment is selected to give the same volume for each segment. This resulted in thinner segments in the outer regions and thicker segments in the inner region. This type of segmentation allows for capturing the skin effect that is discussed before.

The SCHW reactor uses CANFLEX bundle, with 43-elements. The central fuel element and the first ring elements have a larger radius than the fuel elements in the outer two rings. The SCHW utilizes slightly enriched fuel which, which exasperates the end-flux peaking issue. To

suppress the end-flux peaking, the SCHW will utilize two natural uranium fuel pellets at either end of each of the fuel pencils. Furthermore, because of the expected elongation of the fuel cladding, there are four washer and two springs in each fuel elements to absorb some of this elongation, as shown in Figure 5.

The objective of this MCNP model of the half SCHW reactor lattice is to study the end-region power peaking, the impact of the washers and springs on the power distribution and burnup within the bundle and the gas production within the fuel elements. These elements will allow the assessment of whether the bundle can safely operate within the normal and abnormal operating conditions for the SCHW reactor and assess if modifications to the design are needed.

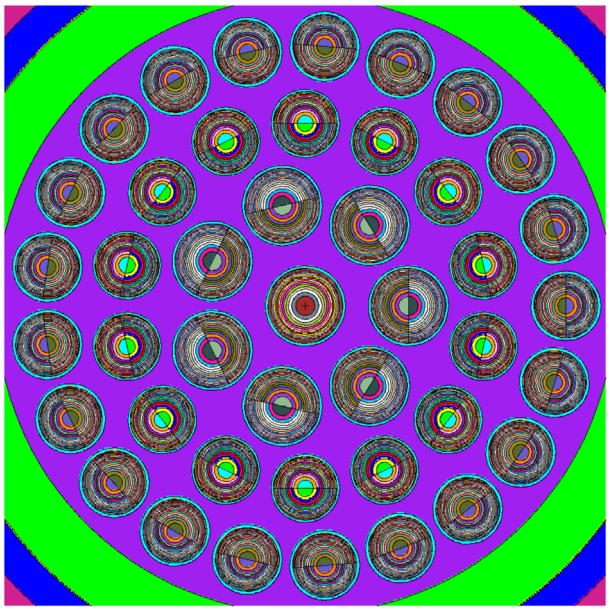

Figure 6: Radial and Angular Segmentation of the Fuel Elements

To capture the flux and power distribution properly in the axial direction, the natural uranium pellet adjacent to the endplate is segmented into four regions. The remaining natural uranium pellet and the following three slightly enriched fuel pellets are segmented into pieces in the axial direction. The objective is to capture the power and flux distribution due to the washers and springs in the fuel pencils.

Beside the radial and angular segmentation of the fuel pencil, the fuel pencil is also segmented in the axial direction. The segmentation is based on obtaining coarse segments at the center of the fuel pencil and finer segmentation at the end-region to capture the impact of the end-region peaking and the washers and springs. The segmentation of the fuel pencil in the axial direction is shown in Figure 5~~Figure 5~~.

4. Flux Distribution Within the Lattice

A static (i.e. No burnup) K-Effective calculation was carried out to show the thermal and fast flux distributions within the half lattice model. This static calculation shows the impact of the

endplate, washers, and springs on the thermal and fast fluxes and power distributions within the half lattice model. As expected, there is increase in the thermal flux at the end plate region due to the additional coolant in the region and dip in the thermal flux around the washers and the springs due to Inconel's high thermal neutron absorption cross-section.

As expected, the thermal flux increases in the end-plate region due to the presence of additional coolant in comparison to the thermal flux at the centre of the bundle, as shown in Figures 7 through 9, respectively. The additional neutron thermalization at the end-plate region causes the end-region peaking in the bundle.

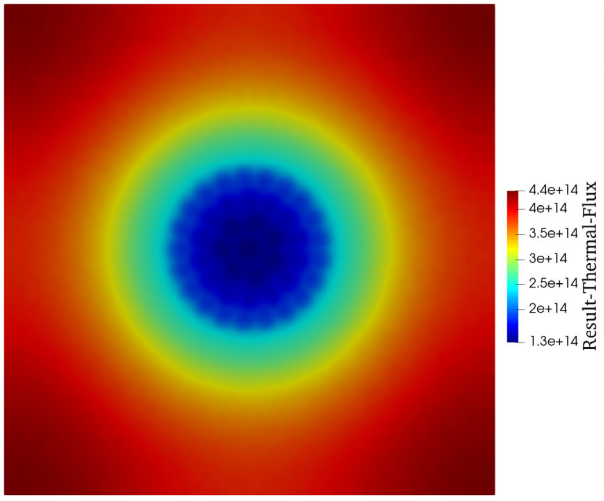

Figure 7: Thermal Flux at the Center of the SCHW Reactor Lattice

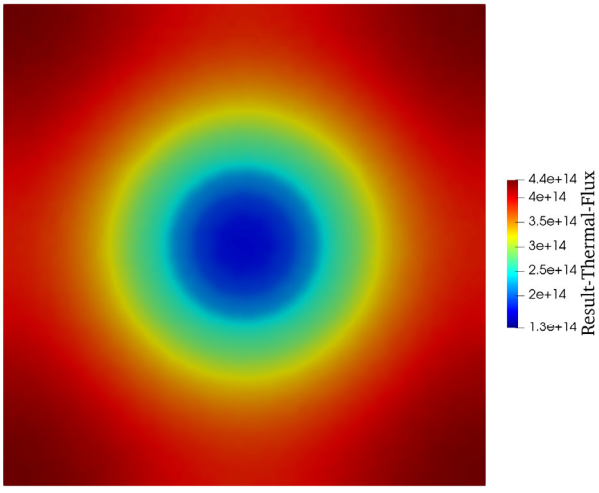

Figure 8: Thermal Flux at the Endplate Region of the SCHW Reactor Lattice

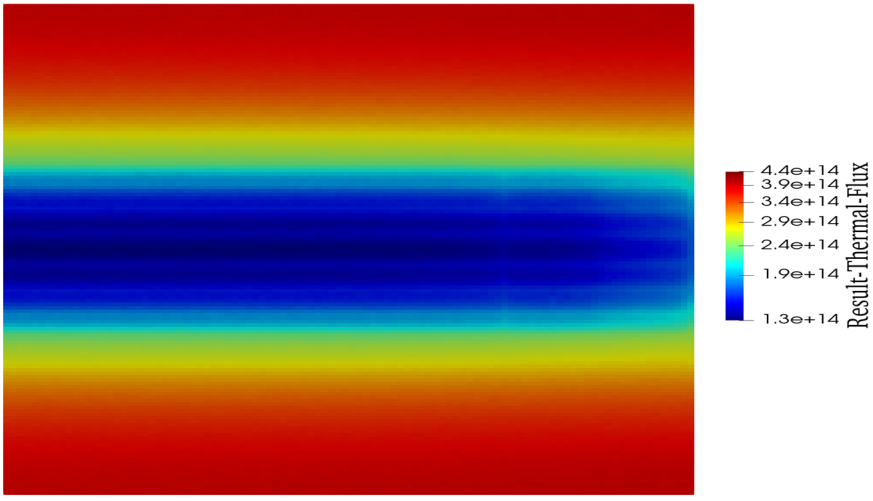

Figure 9: Axial Cross-Section View of the Thermal Flux in the SCHW Reactor Lattice

Figure 10 shows the peaking of the high energy flux at the centre of the fuel bundle due to the fission neutrons born in the fuel elements. There is a noticeable reduction in fast flux at the end region of the bundle due to two different elements. First, the natural uranium pellets, the washers and springs slightly suppress the reactivity and fission in that region of the bundle. Second, the presence of coolant in the endplate region also thermalizes the neutrons and reduces the fast flux in that region. The fast flux at the endplate region and axially across the lattice are shown in Figures 11 and 12, respectively.

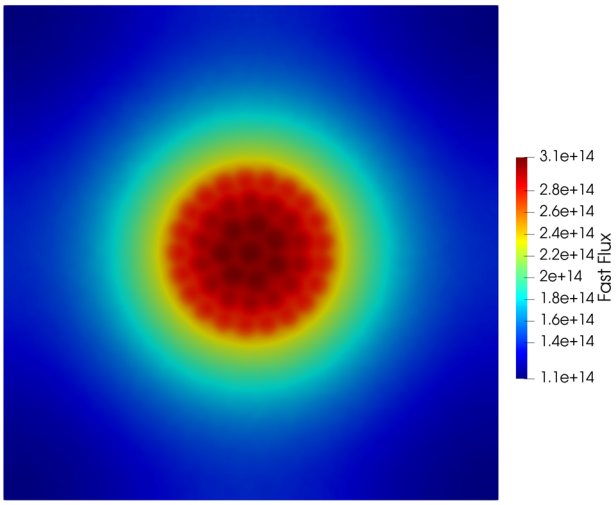

Figure 10: Cross-Section View of the Fast Flux at the Center of the SCHW Reactor Lattice

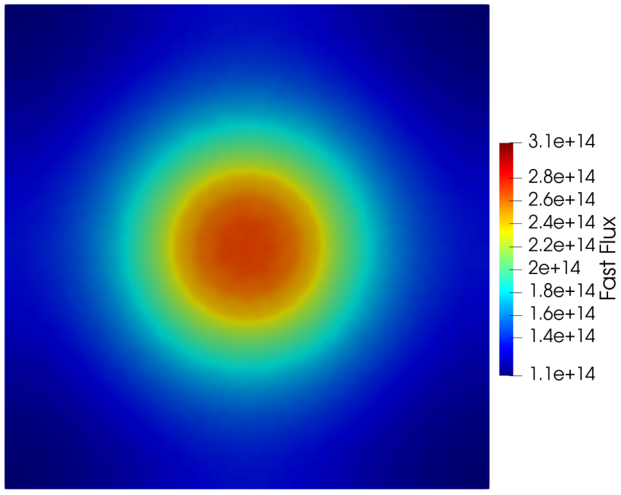

Figure 11: Cross-Section View of the Fast Flux at the Endplate Region of the SCHW Reactor Lattice

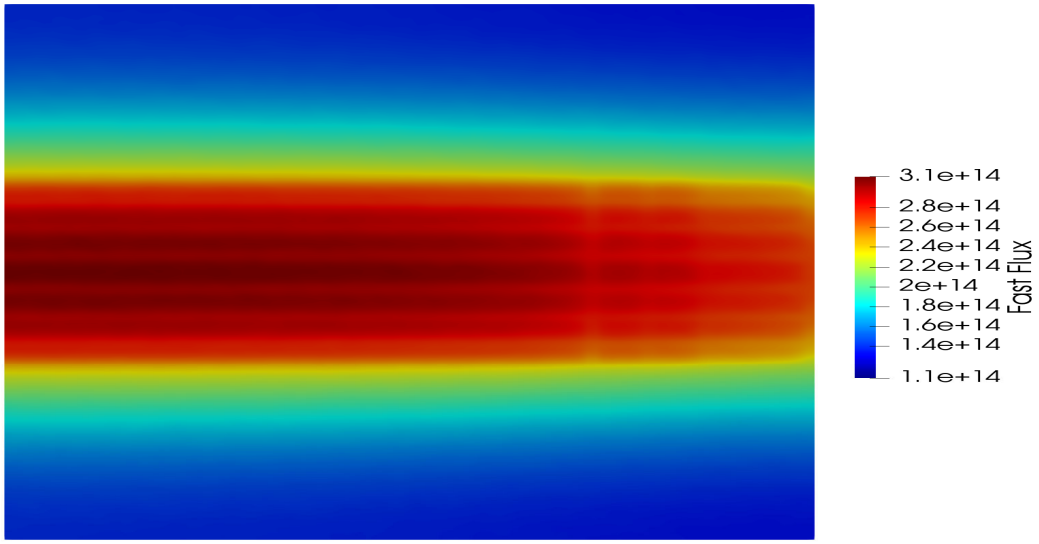

Figure 12: Axial Cross-Section View of the Fast Flux for the SCHW Reactor Lattice

The thermal and fast flux distributions within the SCHW reactor lattice are what is expected.

5. Power Distribution within the Fuel Bundle

Figures 13 and 14 show the power density in the bundle in the axial and radial directions, respectively. There is power suppression at the end region given that natural uranium pellets and washers and springs are in the end-region, close to the endplate, as shown in Figure 13. Beyond the two natural uranium pellets, the power distribution is flat. However, there is a slight increase in the power density towards the end-region of the bundle due to the higher thermal neutrons in that region.

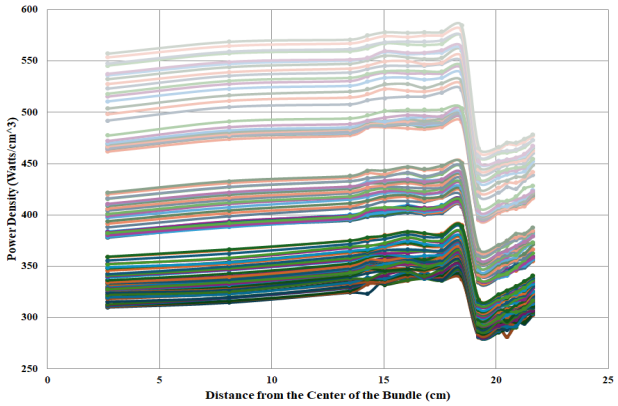

Figure 13: The Power Density Per Burnup Region in the Axial Direction from the Center of the Bundle

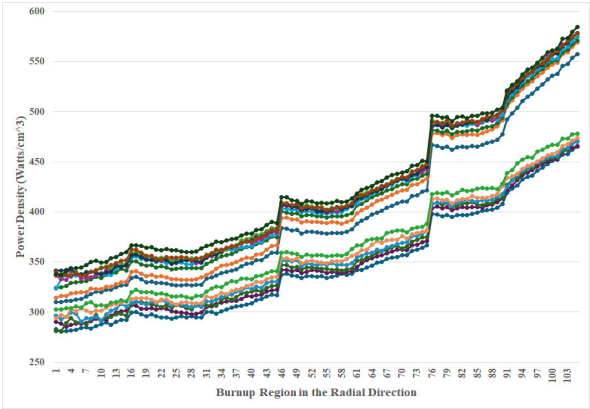

Figure 14: The Power Density Per Burnup Region in the Radial Direction Starting from Central Pin

It is interesting to observe that the highest power density is in the outer fuel element and in the outer region of the outer elements. The power density decreases gradually towards the Centre of the bundle as shown in Figure 14.

The radial power form in terms of the power density at radial locations relative to the power at the centre of the pellet can be derived from the radial segmentation. The power form for the natural uranium fuel pellets in the outer ring of fuel elements is shown in Figure 15 along with the power form derived from a radial profile shape function prediction model [5]. The left-hand side of the plots is the surface of the fuel pellet facing towards the radial centre of the fuel bundle with the right-hand side being for the surface facing outwards, towards the moderator. The MCNP model averages the power density over 180 degrees of azimuth whereas the prediction model has no azimuthal variation. The MCNP model predicts a significantly greater skin effect on the outward facing surface than the inward facing surface.

The radial profile shape function prediction model is based on input parameters of fuel pellet radius, fuel enrichment, burn-up and neutron spectrum. The parameters used for the analysis in Figure 15 are for a fuel pellet radius of 12.15 mm, which is between the inner and outer element pellet radii, natural enrichment, the indicated burn-up, and a CANDU neutron

spectrum [6]. The radial profile shape function prediction provides very similar results to the MCNP calculation for the fuel pellet outward facing surface but predicts a much higher skin effect than is present on the inward facing surface.

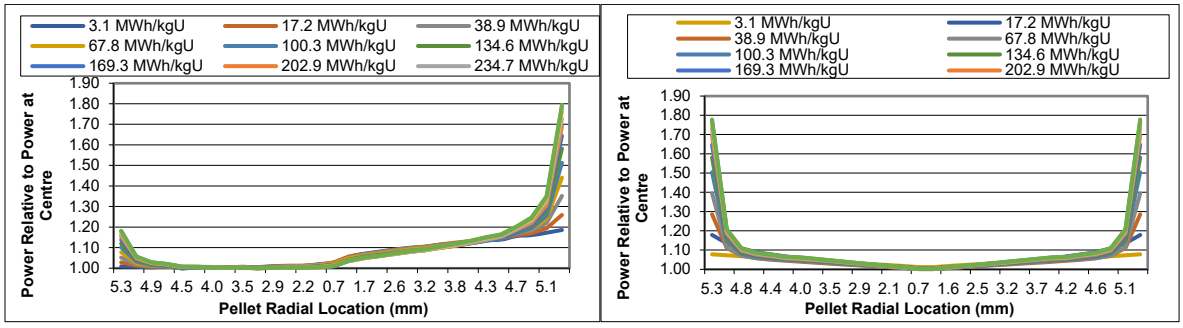

Figure 15: Radial Power Form of Outer Pin Natural Uranium Pellets Compared to Radial Profile Shape Function Prediction Model

The skin effect in the first ring and central elements considerably reduced in comparison to the outer ring of elements as seen in Figure 16. The ring 1 elements have a similar azimuthal asymmetry to the ring 3 elements with the skin effect being higher on the outward facing surface. The central fuel element has an azimuthally uniform power form. The radial profile shape function does not provide representative power forms for the inner elements of the fuel bundle.

The radial power forms can be used to predict fuel temperature distribution and maximum temperature. These are important inputs to fuel behaviour models used to predict fuel pellet thermal deformation and model gaseous fission product migration.

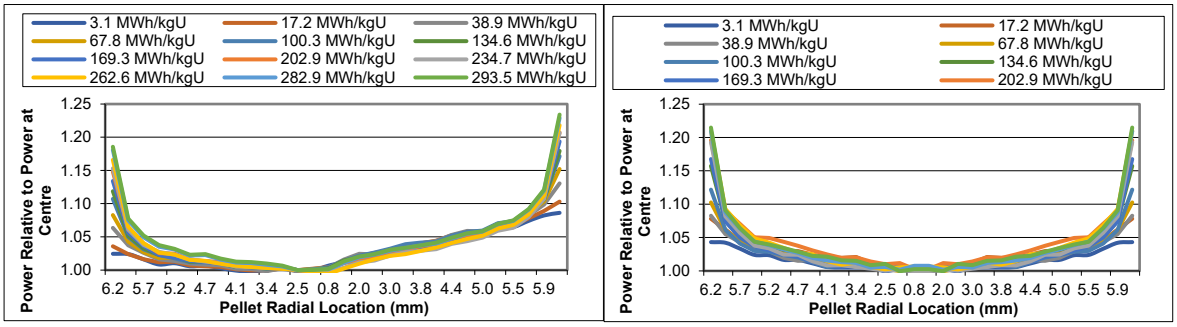

Figure 16: Radial Power Form of Central and First Ring Natural Uranium Pellets

The MCNP model can also predict the spatial concentration of fission product isotopes. Noble gases are of particular interest in fuel modelling due to their potential to migrate to the gap between the fuel pellets and cladding resulting in an increase in pressure of the gap gas. The radial concentration of the noble gas isotopes is provided in Figure 17 for the natural uranium

fuel pellets along with the increase in gas inventory with burn-up. These concentrations and inventories are for the total of isotopes ^{128}Xe, ^{129}Xe, ^{130}Xe, ^{131}Xe, ^{132}Xe, ^{133}Xe, ^{134}Xe, ^{135}Xe, ^{136}Xe, ^{82}Kr, ^{83}Kr, ^{84}Kr, ^{85}Kr and ^{86}Kr and are expressed in terms of Standard Temperature and Pressure (STP) volumes. As can be seen by comparing Figure 17 with Figure 15, the radial and azimuthal form of the isotope concentrations is like the power densities but with a slightly less pronounced skin effect. The noble gas fission product concentration and inventory for the outer fuel ring enriched fuel pellets is shown in Figure 18. The noble gas concentrations are slightly higher in the enriched fuel pellets than the natural ones however the radial and azimuthal distribution is similar.

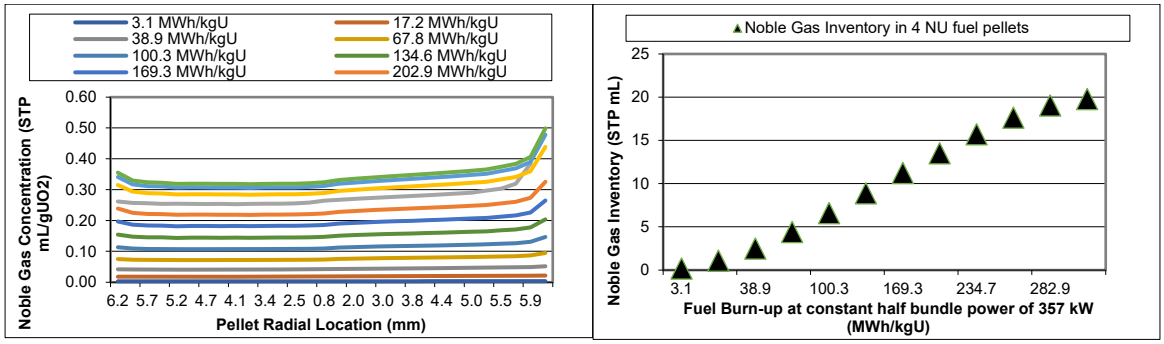

Figure 17: Noble Gas Fission Product Concentration and Inventory in Outer Ring Natural Uranium Fuel Pellets

The total inventory of noble gases in a fuel element is the sum of the inventories in Figures 17 and 18. The noble gases have a non-linear build-up below 100 MWh/kgU, are then approximately linear with burn-up until 250 MWh/kgU and then start to saturate at higher burn-ups.

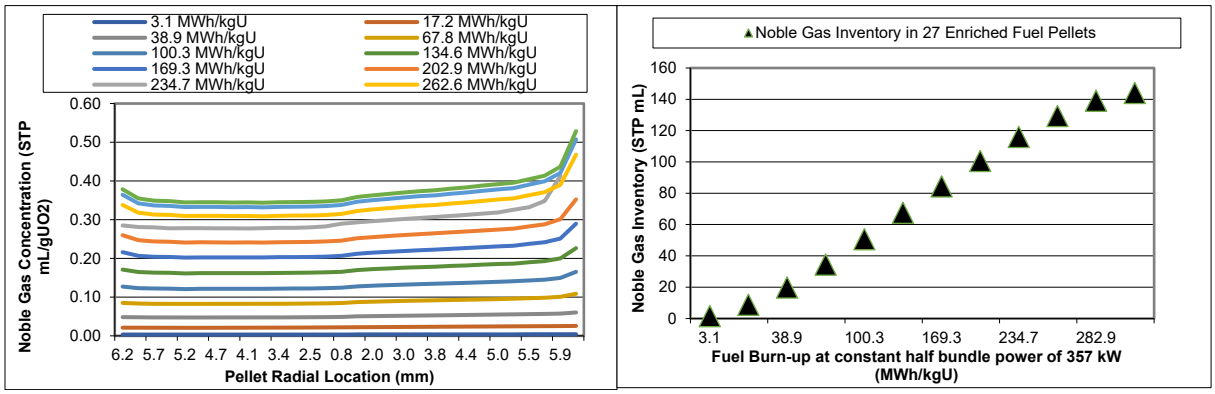

Figure 18: Noble Gas Fission Product Concentration and Inventory in Outer Ring Enriched Uranium Fuel Pellets

6. Conclusions

A detailed MCNP model has been developed for the SCHW reactor with burnup capabilities. This model allows the calculation of power distribution, k-effective, isotopic composition, gas production and flux distribution as function of fuel burnup. The model is flexible enough to allow for changes in state parameters, including coolant density and temperature, moderator density and temperature, fuel enrichment, structural material composition, and components' dimensions.

The predicted k-effective for fresh fuel is 1.183874. The predicted k-effective is going to be sensitive to state parameters, such as coolant density and temperature, moderator density and temperature, and fuel temperature. It is important to understand what the impact of these state parameters on the predicted K-Effective, fuel burnup, gas production and power distribution within the bundle because they will define the boundaries of operation limits for the bundle.

7. References

[1] R.I. Lounsbury, "System design of a refittable supercritical heavy water primary heat transport System for pressurized heavy water reactors", Proceedings of the 42nd Annual Conference of the Canadian Nuclear Society, Saint John, NB, Canada, June 4-7, 2023.

[2] M. Tayal and R. Lounsbury, "Fuel for a supercritical water pressurized heavy water reactor", Proceedings of the 42nd Annual Conference of the Canadian Nuclear Society, Saint John, NB, Canada, June 4-7, 2023.

[3] R.I. Lounsbury, "Development, Qualification Testing and Computer Code Requirements for a Refittable Supercritical Water Primary Heat Transport System", Proceedings of the 43rd Annual Conference of the Canadian Nuclear Society, Saskatoon, SK, Canada, June 16-19, 2024.

[4] Kulesza, Joel, et.al. " MCNP™ Code Version 6.3.0 Theory & User Manual", Los Alamos National Laboratory, Technical Report LA-UR-22-30006, Rev.1, September 2022

[5] Williams, Anthony and Susan Yatabe, "An ANSYS-based 3-Dimensional Thermomechanical Model of a CANDU Fuel Pin", CNL Nuclear Review, Volume 6, Number 2, December 2017.

[6] Gamble, K.A.L., "Modelling Three-Dimensional Deformation Mechanics in CANDU Reactor Fuel Elements", Master of Applied science in Nuclear Engineering, Thesis, Royal Military College of Canada, Kingston, Ontario.